

# 12 Analytical Properties of Self-Energy and Luttinger-Ward Functional

Robert Eder

Institut für Festkörperphysik

Karlsruhe Institute of Technology

## Contents

<b>1</b>	<b>Introduction</b>	<b>2</b>
<b>2</b>	<b>Green function, self-energy, and their analytical properties</b>	<b>2</b>
<b>3</b>	<b>Proof of the theorem by Luttinger and Ward</b>	<b>9</b>
3.1	Statement of the theorem . . . . .	9
3.2	The case $\lambda = 0$ . . . . .	10
3.3	Calculation of $\partial\Omega/\partial\lambda$ . . . . .	11
3.4	Definition and properties of the Luttinger-Ward functional . . . . .	12
3.5	Calculation of $\partial\tilde{\Omega}/\partial\lambda$ . . . . .	18
<b>4</b>	<b>Conserving approximations</b>	<b>20</b>
<b>5</b>	<b>Conclusion</b>	<b>24</b>
<b>A</b>	<b>A theorem on Fourier transforms</b>	<b>25</b>
<b>B</b>	<b>A theorem on determinants</b>	<b>26</b>

## 1 Introduction

In 1961 Luttinger and Ward (LW) published a seminal paper [1] which became the foundation of many important developments in the quantum theory of many particle systems. In particular, they gave an explicit expression for the grand canonical potential  $\Omega$  of an interacting Fermion system. A key step thereby was the construction of the Luttinger-Ward functional, a functional of the Green function which essentially describes the deviation of  $\Omega$  from a non-interacting system. The expression for  $\Omega$  became the basis for the derivation of the famous Luttinger theorem [2], which states that interactions between electrons do not change the volume of the Fermi surface. Subsequently, Baym and Kadanoff [3] investigated the question, under which conditions approximate response functions for systems of interacting particles comply with certain conservation laws, i.e., what is the criterion for the construction of conserving approximations. Baym showed [4] that the Luttinger-Ward functional thereby plays a key role in that a self-energy derived from an approximate Luttinger-Ward functional always gives rise to a conserving approximation. It is the purpose of the present notes to give an introduction to Green functions and the self-energy, derive the LW expression for  $\Omega$  and briefly discuss the ideas of Baym regarding conserving approximations.

## 2 Green function, self-energy, and their analytical properties

In this section we discuss Green functions, their properties and use. Thereby we will also refer to the representation of Green functions in terms of Feynman diagrams but we will not give a derivation of these. Excellent introductions to this subject can be found in various textbooks [5–7]. In the present notes we try to be consistent with Fetter-Walecka (FW) [6].

We consider a system of interacting fermions and assume that there is some complete basis of single-electron states. Each state is labeled by a set of quantum numbers,  $\alpha$ , we denote the number of different sets  $\alpha$  as  $n_\alpha$ . Introducing Fermionic creation/annihilation operators  $c_\alpha^\dagger/c_\alpha$  for electrons in these states, the Hamiltonian, assumed to be time-independent, can be written as  $H = H_0 + H_1$  with

$$H_0 = \sum_{\alpha,\beta} t_{\alpha,\beta} c_\alpha^\dagger c_\beta, \quad (1)$$

$$H_1 = \frac{1}{2} \sum_{\alpha,\beta,\gamma,\delta} V_{\alpha,\beta,\delta,\gamma} c_\alpha^\dagger c_\beta^\dagger c_\gamma c_\delta. \quad (2)$$

Note the factor of  $1/2$  and the ‘inverted’ order of indices on the interaction matrix element  $V$  in (2) which follows from the prescription for second quantization [5–7].  $H$  commutes with the operator  $\hat{N}$  of particle number, which means that eigenstates of  $H$  have a fixed particle number. In all that follows we consider a grand canonical ensemble with inverse temperature  $\beta = 1/k_B T$  and chemical potential  $\mu$ . Introducing  $K = H - \mu N$  the thermal average of any operator  $\hat{O}$  is

$$\langle \hat{O} \rangle_{th} = \frac{1}{Z} \text{Tr} \left( e^{-\beta K} \hat{O} \right)$$

with the grand partition function

$$Z = \text{Tr} (e^{-\beta K}). \quad (3)$$

For any operator  $\hat{O}$  the imaginary time Heisenberg operator is  $\hat{O}(\tau) = e^{\tau K/\hbar} \hat{O} e^{-\tau K/\hbar}$ . Now let  $\hat{A}$  and  $\hat{B}$  be any two operators and  $n_B = [\hat{N}, \hat{B}]$ ,  $n_A = [\hat{N}, \hat{A}]$ . The *imaginary time Green function* then is  $G_{A,B}(\tau, \tau') = -\langle T[\hat{A}(\tau)\hat{B}(\tau')] \rangle_{th}$  where  $T$  is the time-ordering operator. It is easy to see that  $G_{A,B}$  is a function of  $\tau - \tau'$  only and setting  $\tau' = 0$  we find the more explicit expression (with  $\xi_B = (-1)^{n_B}$ )

$$G_{A,B}(\tau) = -\Theta(\tau) \langle \hat{A}(\tau) \hat{B} \rangle_{th} - \xi_B \Theta(-\tau) \langle \hat{B} \hat{A}(\tau) \rangle_{th} \quad (4)$$

$$= \frac{1}{Z} \left( -\Theta(\tau) \sum_{i,j} e^{-\beta K_i} e^{\frac{\tau}{\hbar}(K_i - K_j)} \langle i | \hat{A} | j \rangle \langle j | \hat{B} | i \rangle - \xi_B \Theta(-\tau) \sum_{i,j} e^{-\beta K_i} e^{\frac{\tau}{\hbar}(K_j - K_i)} \langle i | \hat{B} | j \rangle \langle j | \hat{A} | i \rangle \right), \quad (5)$$

Here  $|i\rangle$  are the exact eigenstates of  $H$  and  $K_i = E_i - \mu N_i$  the corresponding eigenvalues of  $K$  with energy  $E_i$  and particle number  $N_i$ . It is obvious from (5) that  $G$  can be different from zero only if  $n_A = -n_B$ . The  $\tau$ -dependence of both terms in (5) is  $e^{(-\beta + \frac{|\tau|}{\hbar})K_i} e^{-\frac{|\tau|}{\hbar}K_j}$ . Since the  $K_i$  are bounded from below (namely by the  $K$  for the ground state with the given  $\mu$ ) but unbounded from above in the thermodynamical limit,  $G$  is well-defined only for  $\tau \in [-\beta\hbar, \beta\hbar]$  [8]. Using the cyclic property of the trace one can show that for  $\tau \in [-\beta\hbar, 0]$  one has  $G(\tau + \beta\hbar) = \xi_B G(\tau)$ . Accordingly,  $G$  can be expanded in a Fourier series

$$G(\tau) = \frac{1}{\beta\hbar} \sum_{\nu=-\infty}^{\infty} e^{-i\omega_\nu \tau} G(i\omega_\nu),$$

$$G(i\omega_\nu) = \int_0^{\beta\hbar} d\tau e^{i\omega_\nu \tau} G(\tau), \quad (6)$$

with  $\omega_\nu = \frac{\nu\pi}{\beta\hbar}$  and integer  $\nu$ . The  $\omega_\nu$  are called Matsubara frequencies and for even  $n_B$  (odd  $n_B$ ) only even  $\nu$  (odd  $\nu$ ) contribute in the Fourier expansion. Using (5) one finds

$$G_{A,B}(i\omega_\nu) = \frac{1}{Z} \sum_{i,j} \frac{e^{-\beta K_i} - \xi_B e^{-\beta K_j}}{i\omega_\nu + \frac{1}{\hbar}(K_i - K_j)} \langle i | \hat{A} | j \rangle \langle j | \hat{B} | i \rangle. \quad (7)$$

Next, we consider the retarded real-time Green function. The real-time Heisenberg operator is  $\hat{O}(\tau) = e^{itK/\hbar} \hat{O} e^{-itK/\hbar}$  and the retarded real-time Green function is

$$G_{A,B}^R(t) = -i\Theta(t) \left( \langle \hat{A}(t) \hat{B} \rangle_{th} - \xi_B \langle \hat{B} \hat{A}(t) \rangle_{th} \right). \quad (8)$$

It is straightforward to write down the expression of  $G_{A,B}^R(t)$  corresponding to (5), and using the theorem in Appendix A one finds its Fourier transform

$$G_{A,B}^R(\omega) = \frac{1}{Z} \lim_{\eta \rightarrow 0^+} \sum_{i,j} \frac{e^{-\beta K_i} - \xi_B e^{-\beta K_j}}{\omega + i\eta + \frac{1}{\hbar}(K_i - K_j)} \langle i | \hat{A} | j \rangle \langle j | \hat{B} | i \rangle. \quad (9)$$

Comparing with (7) it is obvious that  $G_{A,B}^R(\omega)$  can be obtained from  $G_{A,B}(i\omega_\nu)$  by replacing  $i\omega_\nu \rightarrow \omega + i0^+$ . In other words, there is one function  $G_{A,B}(z)$  of the complex variable  $z$  – usually called ‘the’ Green function – which gives  $G_{A,B}(i\omega_\nu)$  when it is evaluated for the Matsubara frequencies, and  $G_{A,B}^R(\omega)$  when it is evaluated along a line infinitesimally above the real axis. Equation (7) is the *Lehmann representation* of the Green function. The existence of ‘the’ Green function is the very reason why the imaginary time Green function is so useful. In principle, the quantity of physical interest is the real-time Green function. For example one can show that if a system is acted upon by a time dependent perturbation of the form  $H_p = f(t)\hat{B}$  (with  $\hat{B}$  some Hermitean operator and  $f(t)$  a real function), the change of the expectation value of some operator  $\hat{A}$  which is linear in  $f(t)$  is given by (see FW (32.2))

$$\delta \langle \hat{A} \rangle(t) = \frac{1}{\hbar} \int_{-\infty}^{\infty} dt' G_{AB}^R(t-t')f(t').$$

On the other hand, the imaginary-time Green function can be evaluated approximately by using the powerful technique of expansion in Feynman diagrams [5–7], which is *not* possible for the real-time Green functions. The standard way to obtain the real-time Green function, which is used over and over again in the literature, is to first obtain an approximate  $G_{A,B}(i\omega_\nu)$  by doing an expansion in Feynman diagrams and then continue this analytically to a line infinitesimally above the real axis to obtain the real-time Green function of physical interest.

We now specialize to the *single-particle Green function* which corresponds to  $\hat{A} = c_\alpha$ ,  $\hat{B} = c_\beta^\dagger$  (so that  $\xi_B = -1$ ). It may be viewed as a matrix of dimension  $n_\alpha \times n_\alpha$ , denoted by  $\mathbf{G}$ , and we can write it

$$G_{\alpha,\beta}(z) = \frac{1}{Z} \sum_{i,j} e^{-\beta K_i} \left[ \frac{\langle i|c_\beta^\dagger|j\rangle\langle j|c_\alpha|i\rangle}{z - (K_i - K_j)/\hbar} + \frac{\langle i|c_\alpha|j\rangle\langle j|c_\beta^\dagger|i\rangle}{z - (K_j - K_i)/\hbar} \right], \quad (10)$$

$$= \int_{-\infty}^{\infty} d\omega \frac{\rho_{\alpha,\beta}^{(-)}(\omega)}{z - \omega} + \int_{-\infty}^{\infty} d\omega \frac{\rho_{\alpha,\beta}^{(+)}(\omega)}{z - \omega} \quad (11)$$

$$\rho_{\alpha,\beta}^{(-)}(\omega) = \frac{1}{Z} \sum_{i,j} e^{-\beta K_i} \langle i|c_\beta^\dagger|j\rangle\langle j|c_\alpha|i\rangle \delta(\omega - (K_i - K_j)/\hbar), \quad (12)$$

$$\rho_{\alpha,\beta}^{(+)}(\omega) = \frac{1}{Z} \sum_{i,j} e^{-\beta K_i} \langle i|c_\alpha|j\rangle\langle j|c_\beta^\dagger|i\rangle \delta(\omega - (K_j - K_i)/\hbar). \quad (13)$$

Since  $K_j - K_i$  is real,  $\mathbf{G}(z)$  has a number of poles on the real axis. For both,  $\rho^{(-)}$  and  $\rho^{(+)}$ , one has  $\rho_{\alpha,\beta}^*(\omega) = \rho_{\beta,\alpha}(\omega)$  i.e., the  $\omega$ -dependent matrix  $\boldsymbol{\rho}(\omega)$  is Hermitean. Moreover, for any vector  $\mathbf{v}$  of length  $n_\alpha$  we have

$$\sum_{\alpha,\beta} v_\alpha^* \rho_{\alpha,\beta}^{(-)}(\omega) v_\beta = \frac{1}{Z} \sum_{i,j} e^{-\beta K_i} |\langle j|c_{\mathbf{v}}|i\rangle|^2 \delta(\omega - (K_i - K_j)/\hbar) > 0$$

with  $c_{\mathbf{v}} = \sum v_\alpha c_\alpha$  so that  $\boldsymbol{\rho}$  are positive definite. It follows from the Hermiticity of  $\boldsymbol{\rho}$  that  $[\mathbf{G}(z)]^+ = \mathbf{G}(z^*)$  which shows that, for complex  $z$ ,  $\mathbf{G}(z)$  is *not* Hermitean.

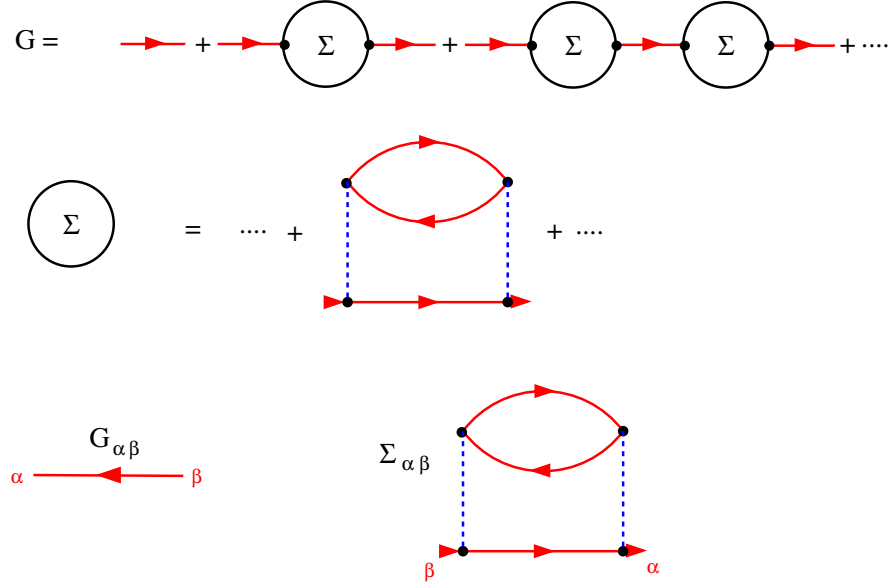


**Fig. 1:** *Top: Graphical representation of the Dyson equation. Middle: Self-energy diagrams have two open ends. Bottom: The convention for the representation of the Green function implies the labeling of the open ends of the self-energy.*

We now assume that the range of  $\omega$  where the elements of  $\rho^{(\pm)}$  are different from zero is finite, which means that the change in energy upon adding or removing an electron is bounded. Then we consider the limit  $|z| \rightarrow \infty$  and expand

$$\frac{1}{z \pm (K_j - K_i)/\hbar} \rightarrow \frac{1}{z} \mp \frac{K_j - K_i}{\hbar z^2} + O\left(\frac{1}{z^3}\right).$$

Inserting this into (10) and using  $(K_j - K_i)\langle j|c_\alpha|i\rangle = \langle j|[K, c_\alpha]|i\rangle$  we find

$$G_{\alpha,\beta}(z) \rightarrow \frac{\delta_{\alpha,\beta}}{z} + \frac{\left\langle \left\{ c_\beta^\dagger, [c_\alpha, K] \right\} \right\rangle_{th}}{\hbar z^2} + O\left(\frac{1}{z^3}\right).$$

Using the Hamiltonian (1) and (2) one finds

$$\left\langle \left\{ c_\beta^\dagger, [c_\alpha, K] \right\} \right\rangle_{th} = t_{\alpha,\beta} - \mu \delta_{\alpha,\beta} + \sum_{\gamma,\delta} (V_{\alpha,\gamma,\beta,\delta} - V_{\alpha,\gamma,\delta,\beta}) \langle c_\gamma^\dagger c_\delta \rangle_{th}. \quad (14)$$

The term involving  $V$  ‘looks like’ the Hartree-Fock potential  $V_{\alpha,\beta}^{(HF)}$ , however, whereas for the true Hartree-Fock potential the thermal average has to be taken using the Hartree-Fock wave functions and energies, the thermal average in (14) has to be taken using the fully interacting eigenstates and energies. Keeping this subtle difference in mind we still call the third term the Hartree-Fock potential  $V_{\alpha,\beta}^{(HF)}$  so that

$$\mathbf{G}(z) \rightarrow \frac{1}{z} + \frac{\mathbf{t} - \mu + \mathbf{V}^{(HF)}}{\hbar z^2} + O\left(\frac{1}{z^3}\right). \quad (15)$$

As already mentioned the imaginary-time Green function can be expanded in Feynman diagrams and the self-energy  $\Sigma(i\omega_\nu)$  be introduced in the standard way see Figure 1. The self-energy can be expanded in diagrams which have two ‘entry points’ an incoming and an outgoing one. Following FW [6] we represent the Green function  $G_{\alpha\beta}$  and also the noninteracting Green function  $G_{\alpha\beta}^0$  by a directed line with an arrow running  $\beta \rightarrow \alpha$  (the reason is, that it is the *creation operator* which has the index  $\beta$ , see (10)). In the Dyson equation the matrix indices of the Green function and the self-energy must take the form of consecutive matrix products, e.g.,  $G_{\delta\alpha}^0 \Sigma_{\alpha\beta} G_{\beta\gamma}^0$  – otherwise the summation of the geometric series would not be possible. It follows that the element  $\Sigma_{\alpha\beta}$  must have the label  $\alpha$  on the outgoing entry and the label  $\beta$  on the incoming one, see Figure 1. The diagrammatic expansion shows [5–7] that the Green function obeys the Dyson equation

$$\begin{aligned} \left( i\omega_\nu - \frac{1}{\hbar} (\mathbf{t} - \mu) - \Sigma(i\omega_\nu) \right) \mathbf{G}(i\omega_\nu) &= 1 \\ \left( -\partial_\tau - \frac{1}{\hbar} (\mathbf{t} - \mu) \right) \mathbf{G}(\tau) - \int_0^{\beta\hbar} \Sigma(\tau - \tau') \mathbf{G}(\tau') d\tau' &= \delta(\tau), \end{aligned} \quad (16)$$

where the second equation is the Fourier-transform of the first and FW (25.21) was used. The inverse of the Green function thus is

$$\mathbf{G}^{-1}(z) = z - \frac{1}{\hbar} (\mathbf{t} - \mu) - \Sigma(z)$$

On the other hand, from (15) we find

$$\mathbf{G}^{-1}(z) \rightarrow z - \frac{\mathbf{t} - \mu}{\hbar} - \frac{\mathbf{V}^{(HF)}}{\hbar} + O\left(\frac{1}{z}\right) \Rightarrow \Sigma(z) \rightarrow \frac{\mathbf{V}^{(HF)}}{\hbar} + O\left(\frac{1}{z}\right).$$

Accordingly, the quantity  $\bar{\Sigma} = \Sigma - \mathbf{V}^{(HF)}$  vanishes as  $1/z$  for large  $|z|$ .

Next, let  $\mathbf{v}$  be any complex vector of length  $n_\alpha$  and consider

$$f(z) = \sum_{\alpha,\beta} v_\alpha^* G_{\alpha,\beta}(z) v_\beta = \frac{1}{Z} \sum_{i,j} \frac{e^{-\beta K_i} + e^{-\beta K_j}}{z + (K_i - K_j)/\hbar} |\langle j | c_\mathbf{v}^\dagger | i \rangle|^2, \quad (17)$$

where  $c_\mathbf{v}^\dagger = \sum v_\alpha c_\alpha^\dagger$  and we have used (7). Putting  $z = x + iy$  the imaginary part reads

$$\mathcal{I}f(z) = -\frac{y}{Z} \sum_{i,j} \frac{e^{-\beta K_i} + e^{-\beta K_j}}{(x + (K_i - K_j)/\hbar)^2 + y^2} |\langle j | c_\mathbf{v}^\dagger | i \rangle|^2.$$

This expression cannot be zero unless  $y = 0$ . It follows that for  $z$  away from the real axis all eigenvalues of  $\mathbf{G}(z)$  are different from zero [9], otherwise we might choose  $\mathbf{v}$  to be either the right- or left-hand eigenvector for eigenvalue 0 and obtain  $f(z) = 0$  (note that for complex  $z$   $\mathbf{G}(z)$  is not Hermitian which means that right- and left-hand eigenvectors will be different). In fact, this is the very condition that  $\mathbf{G}^{-1}(z)$  does exist and it follows that for all complex  $z$  the determinant of  $\mathbf{G}(z)$  is different from zero. Using Cramer’s rule we find the elements of the inverse Green function

$$G_{\alpha,\beta}^{-1}(z) = \frac{(-1)^{\alpha+\beta} \det \mathbf{M}_{\alpha,\beta}(z)}{\det \mathbf{G}(z)},$$

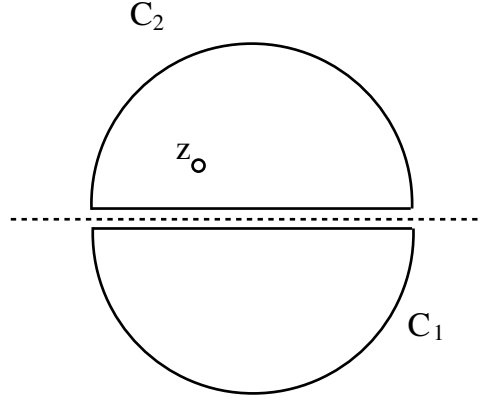


**Fig. 2:** Integration contours for the proof of the spectral representation of  $\bar{\Sigma}$ . The dashed line is the real  $z'$  axis.

where  $M_{\alpha,\beta}(z)$  is the respective minor of  $\mathbf{G}(z)$ , i.e., the matrix  $\mathbf{G}(z)$  with row  $\alpha$  and column  $\beta$  discarded. Since for  $z$  away from the real axis all elements of  $\mathbf{G}(z)$  are finite, see Eq. 10, and the determinant of  $\mathbf{G}(z)$  different from zero it follows that away from the real axis all elements of  $\mathbf{G}^{-1}(z)$  are analytical functions of  $z$ . Starting from  $\mathbf{G}^{-1}(z)\mathbf{G}(z) = 1$ , taking the Hermitean conjugate and using  $[\mathbf{G}(z)]^+ = \mathbf{G}(z^*)$  we find  $[\mathbf{G}^{-1}(z)]^+ = \mathbf{G}^{-1}(z^*)$ . Since both,  $(\mathbf{G}^0)^{-1}(z) = z - (\mathbf{t} - \mu)/\hbar$  and  $\mathbf{V}^{HF}$ , obey this relation, it follows that  $\bar{\Sigma}(z)$  alone obeys this relation as well, i.e.,  $\bar{\Sigma}(z^*) = \bar{\Sigma}^+(z)$ . For real  $\omega$ , we define the real matrices  $\mathbf{K}(\omega)$  and  $\mathbf{J}(\omega)$  by

$$\bar{\Sigma}(\omega + i0^+) = \mathbf{K}(\omega) + i\mathbf{J}(\omega) \Rightarrow \bar{\Sigma}(\omega - i0^+) = \mathbf{K}^T(\omega) - i\mathbf{J}^T(\omega). \quad (18)$$

Next, we define

$$\begin{aligned} \bar{\Sigma}^{(+)}(z) &= \frac{1}{2} (\bar{\Sigma}(z) + \bar{\Sigma}^T(z)) \Rightarrow \bar{\Sigma}^{(+)}(\omega \pm i0^+) = \mathbf{K}^{(+)}(\omega) \pm i\mathbf{J}^{(+)}(\omega), \\ \bar{\Sigma}^{(-)}(z) &= \frac{i}{2} (\bar{\Sigma}(z) - \bar{\Sigma}^T(z)) \Rightarrow \bar{\Sigma}^{(-)}(\omega \pm i0^+) = -\mathbf{J}^{(-)}(\omega) \pm i\mathbf{K}^{(-)}(\omega), \end{aligned} \quad (19)$$

where  $\mathbf{K}^{(\pm)} = \frac{1}{2}(\mathbf{K} \pm \mathbf{K}^T)$  and  $\mathbf{J}^{(\pm)} = \frac{1}{2}(\mathbf{J} \pm \mathbf{J}^T)$ . Now consider the integration contours in Figure 2 which consist of lines infinitesimally above and below the real axis and semicircles at infinity. Since  $\bar{\Sigma}$  is analytic away from the real axis we have for  $z$  in the upper half-plane

$$\oint_{C_1} dz' \frac{\bar{\Sigma}^{(\pm)}(z')}{z' - z} = 0 \Rightarrow \int_{-\infty}^{\infty} d\omega \frac{\mathbf{K}^{(\pm)}(\omega)}{\omega - z} = i \int_{-\infty}^{\infty} d\omega \frac{\mathbf{J}^{(\pm)}(\omega)}{\omega - z}.$$

The second equation follows, because the integrand is  $\propto 1/z'^2$  for large  $|z'|$  so that the arc does not contribute and infinitesimally below the real axis we can use (18). Next we can use Cauchy's theorem and write

$$\bar{\Sigma}^{(\pm)}(z) = \frac{1}{2\pi i} \oint_{C_2} dz' \frac{\bar{\Sigma}^{(\pm)}(z')}{z' - z} \Rightarrow \bar{\Sigma}^{(\pm)}(z) = \pm \frac{1}{\pi} \int_{-\infty}^{\infty} d\omega \frac{\mathbf{J}^{(\pm)}(\omega)}{\omega - z}.$$

Reverting (19) and recalling the definition of  $\bar{\Sigma}$  we finally arrive at the spectral representation of the self-energy, as derived by Luttinger [10]

$$\Sigma(z) = \mathbf{V}^{(HF)} + \frac{1}{\pi} \int_{-\infty}^{\infty} d\omega \frac{\boldsymbol{\sigma}(\omega)}{\omega - z} \quad (20)$$

with  $\boldsymbol{\sigma}(\omega) = \mathbf{J}^{(+)}(\omega) + i\mathbf{J}^{(-)}(\omega)$ , which shows that  $\boldsymbol{\sigma}(\omega)$  is Hermitean. It should be noted that in deriving (20) we have made use only of the Dyson equation and certain rigorous analytical properties of the Green function. This is therefore a completely rigorous result. It should also be noted that we have shown that for any  $z$  off the real axis  $\mathbf{G}^{-1}(z)$  is well-defined. This shows that there is a unique mapping  $\mathbf{G}(z) \rightarrow \Sigma(z)$ .

We have introduced the self-energy using the diagrammatic expansion of the Green function but it can also be defined in another way. Using  $-\hbar\partial_{\tau}\hat{O} = [\hat{O}, K]$  and  $\partial_{\tau}\Theta(\pm\tau) = \pm\delta(\tau)$  we find the equation of motion of the imaginary time Green function:

$$-\hbar\partial_{\tau}G_{\alpha,\beta}(\tau) = \hbar\delta_{\alpha,\beta}\delta(\tau) + \sum_{\nu} (t_{\alpha,\nu} - \mu\delta_{\alpha,\nu})G_{\nu,\beta}(\tau) - \sum_{\nu,\kappa,\lambda} V_{\alpha,\nu,\kappa,\lambda} \langle T[(c_{\nu}^{\dagger}c_{\lambda}c_{\kappa})(\tau)c_{\beta}^{\dagger}(0)] \rangle_{th}$$

The time-ordered product in the last term can be written as  $G_2(\lambda\tau, \kappa\tau, \beta 0, \nu\tau^+)$  where

$$G_2(\lambda\tau_1, \kappa\tau_2, \beta\tau_3, \nu\tau_4) = (-1)^2 \langle T[c_{\lambda}(\tau_1)c_{\kappa}(\tau_2)c_{\nu}^{\dagger}(\tau_4)c_{\beta}^{\dagger}(\tau_3)] \rangle_{th}$$

is the two-particle imaginary time Green function (the factor of  $(-1)^2$  has to be replaced by  $(-i)^2$  for the real-time Green function—it is always the square of the prefactor of the single-particle Green function). Comparing with the Dyson equation (16) it is obvious that  $G_2$  and  $\Sigma$  are related as

$$-\sum_{\nu,\kappa,\lambda} V_{\alpha,\nu,\kappa,\lambda} G_2(\lambda\tau, \kappa\tau, \beta 0, \nu\tau^+) = \hbar \int_0^{\hbar\beta} d\tau' \Sigma_{\alpha,\gamma}(\tau-\tau') G_{\gamma,\beta}(\tau'). \quad (21)$$

Frequently an approximate Green function is found by expressing  $G_2$  as a functional of  $G$ . For example, the Hartree-Fock approximation corresponds to replacing

$$G_2(\lambda\tau_1, \kappa\tau_2, \beta\tau_3, \nu\tau_4) \rightarrow G(\lambda\tau_1, \beta\tau_3)G(\kappa\tau_2, \nu\tau_4) - G(\lambda\tau_1, \nu\tau_4)G(\kappa\tau_2, \beta\tau_3).$$

Inserting this into (21) one obtains

$$\begin{aligned} -\sum_{\nu,\kappa,\lambda} V_{\alpha,\nu,\kappa,\lambda} G_2(\lambda\tau, \kappa\tau, \beta 0, \nu\tau^+) &= \sum_{\nu,\kappa,\lambda} (V_{\alpha,\nu,\lambda,\kappa} - V_{\alpha,\nu,\kappa,\lambda}) \langle c_{\nu}^{\dagger}c_{\kappa} \rangle G_{\lambda,\beta}(\tau) \\ &\Rightarrow \Sigma_{\alpha,\nu}(\tau) = \frac{1}{\hbar} V_{\alpha,\nu}^{(HF)} \delta(\tau) \end{aligned}$$

which is what one would have expected for the self-energy in Hartree-Fock approximation.



### 3 Proof of the theorem by Luttinger and Ward

#### 3.1 Statement of the theorem

In the present section we consider a solid, described by an LCAO-like Hamiltonian. Then we have  $\alpha = (i, n, \nu, \sigma)$  where  $i \in \{1, \dots, N\}$  denotes the unit cell,  $n \in \{1, \dots, n_{Atom}\}$  the number of atoms in the basis,  $\nu \in \{s, p_x, p_y, p_z, d_{xy} \dots\}$  the type of orbital and  $\sigma$  the  $z$ -component of spin. The number of all orbitals in the unit cell is  $n_{orb}$ . The Fourier transform of the Fermion operators is

$$c_{\mathbf{k},\beta}^\dagger = \frac{1}{\sqrt{N}} \sum_i e^{i\mathbf{k} \cdot (\mathbf{R}_i + \mathbf{r}_n)} c_{i,n,\nu,\sigma}^\dagger,$$

where we have introduced the orbital index  $\beta = (n, \nu, \sigma)$ . Since this second compound index always comes together with either a momentum  $\mathbf{k}$  or a cell index  $i$ , no misunderstanding is possible. The Hamiltonian now can be written as

$$H_0 = \sum_{\mathbf{k}} \sum_{\alpha,\beta} t_{\alpha,\beta}(\mathbf{k}) c_{\mathbf{k},\alpha}^\dagger c_{\mathbf{k},\beta}, \quad (22)$$

$$H_1 = \frac{1}{2} \sum_{\mathbf{k},\mathbf{k}',\mathbf{q}} \sum_{\alpha,\beta,\gamma,\delta} V_{\alpha,\beta,\delta,\gamma}(\mathbf{k},\mathbf{k}',\mathbf{q}) c_{\mathbf{k}+\mathbf{q},\alpha}^\dagger c_{\mathbf{k}'-\mathbf{q},\beta}^\dagger c_{\mathbf{k}',\gamma} c_{\mathbf{k},\delta}. \quad (23)$$

Equation (22) defines the  $2n_{orb} \times 2n_{orb}$  matrix  $\mathbf{t}(\mathbf{k})$ , whose eigenvalues  $E_n(\mathbf{k})$  give the noninteracting band structure. This formulation allows  $H_0$  to describe magnetic systems or include spin-orbit coupling.

The grand canonical potential  $\Omega(T, \mu)$  contains all thermodynamical information about a system at fixed temperature  $T$  and chemical potential  $\mu$ . It is defined as the logarithm of the grand partition function

$$\Omega = -\frac{1}{\beta} \ln(Z) \quad \text{with} \quad Z = \sum_i e^{-\beta(E_i - \mu N_i)},$$

where the sum is over all eigenstates of the system with energy  $E_i$  and particle number  $N_i$ . The latter can indeed be evaluated for noninteracting particles and in this way one obtains for example the grand canonical potential of noninteracting Bloch electrons

$$\Omega = -\frac{1}{\beta} \sum_{n=1}^{2n_{orb}} \sum_{\mathbf{k}} \ln(1 + e^{-\beta(E_n(\mathbf{k}) - \mu)}). \quad (24)$$

As shown in textbooks of statistical mechanics, expression (24) allows to derive the complete thermodynamics of metals. However, it is in general not possible to evaluate the grand partition function for a system of *interacting particles* of macroscopic size.

Luttinger and Ward, however, derived a relation for the grand canonical potential of interacting Fermions [1]. More precisely, they considered the following quantity

$$\Omega' = -\lim_{\eta \rightarrow 0^+} \frac{1}{\beta} \sum_{\mathbf{k},\nu} e^{i\omega_\nu \eta} \left( \ln \det(-\mathbf{G}^{-1}(\mathbf{k}, i\omega_\nu)) + \text{Tr}(\mathbf{G}(\mathbf{k}, i\omega_\nu) \boldsymbol{\Sigma}(\mathbf{k}, i\omega_\nu)) \right) + \Phi[\mathbf{G}]. \quad (25)$$

Here  $\sum_\nu$  denotes summation over the Fermionic Matsubara frequencies and  $\Phi[\mathbf{G}]$  is the so-called Luttinger-Ward functional which is defined as a sum over closed, linked Feynman-diagrams (the precise definition will be discussed below). The important point here is that a closed Feynman diagram is simply a number, so that  $\Phi[\mathbf{G}]$  indeed assigns a (real) number to each possible Green function  $\mathbf{G}$ . As regards the logarithm of the determinant in (25) we recall that the determinant of a matrix is given by the product of its eigenvalues (the matrix need not be Hermitean for this to be true) so that the logarithm of the determinant is the sum of the logarithms of the (complex) eigenvalues of  $-\mathbf{G}^{-1}$ .

In the following we want to show that in fact  $\Omega' = \Omega$ , the true grand canonical potential, and thereby follow the original proof by Luttinger and Ward. The basic idea is to multiply the interaction part of the Hamiltonian, (2), by a scale factor,  $H_1 \rightarrow \lambda H_1$ , then show  $\Omega' = \Omega$  for  $\lambda = 0$ , i.e., the noninteracting limit, and next show that  $\partial_\lambda \Omega' = \partial_\lambda \Omega$ . Obviously, this proves the identity of the two expressions for any  $\lambda$ .

### 3.2 The case $\lambda = 0$

In this limit  $\Sigma = 0$  and  $\Phi[\mathbf{G}] = 0$  (the latter property follows because all interaction lines in all diagrams are zero) so that only the first term in (25) remains and

$$\begin{aligned} \mathbf{G}^{-1}(\mathbf{k}, \omega) &= \omega + (\mu - \mathbf{t}(\mathbf{k})) / \hbar, \\ \ln \det(-\mathbf{G}^{-1}(\mathbf{k}, \omega)) &= \sum_{n=1}^{2n_{orb}} \ln \left( -\omega - (\mu - E_n(\mathbf{k})) / \hbar \right). \end{aligned} \quad (26)$$

We now replace the sum over Matsubara frequencies by a contour integration, which is a standard trick used in field theory (see, e.g., section 25 of FW) and obtain

$$-\frac{1}{\beta} \sum_\nu e^{i\omega_\nu \eta} \ln \det(-\mathbf{G}^{-1}(\mathbf{k}, i\omega_\nu)) = \frac{\hbar}{2\pi i} \oint_{\mathcal{C}} d\omega f(\omega) e^{\omega \eta} \ln \det(-\mathbf{G}^{-1}(\mathbf{k}, \omega)) \quad (27)$$

where

$$f(\omega) = \frac{1}{e^{\beta \hbar \omega} + 1},$$

is the Fermi function and the contour  $\mathcal{C}$  encircles the imaginary axis in counterclockwise fashion, see Figure 3(a). Next we note that the integrals along the two clover-shaped contours in Figure 3(b) are zero, *provided* the integrand is analytic in the interior of the two curves. Since the Fermi function has all of its poles along the imaginary axis, which is outside of the curves in Figure 3(b), we only need to consider possible singularities of  $\ln \det(-\mathbf{G}^{-1}(\mathbf{k}, \omega))$ . In principle, the complex logarithm has a branch-cut along the negative real axis which could be problematic. However, a quick glance at (26) shows, that as long as  $\omega$  has a nonvanishing imaginary part, the argument of the logarithm can never be purely real. Singularities of the logarithm thus occur only on the real axis, which also is exterior to the contours in Figure 3(b). The integral along the contours in Figure 3(b) therefore is indeed zero. Next, Jordan's lemma

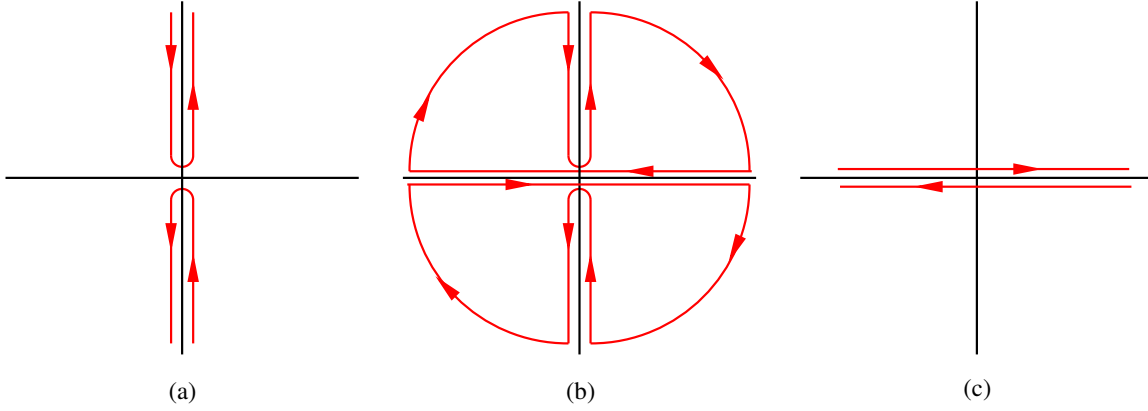


**Fig. 3:** (a) Integration contour  $\mathcal{C}$  used in (27). Since the integrals along the two contours in (b) are zero and the contributions from the circular arcs vanish, the integral along the contour in (a) is equal to that over the contour  $\mathcal{C}'$  in (c).

can be invoked to establish that the integral along the large semicircles vanishes. Here the Fermi function  $f(\omega)$  guarantees that the contribution from the semicircle with  $\text{Re}(\omega) > 0$  vanishes, whereas the factor  $e^{\omega\eta}$  does the same for the semicircle with  $\text{Re}(\omega) < 0$ . It follows that the integral along the contour  $\mathcal{C}$  in Figure 3a is equal to that along the contour  $\mathcal{C}'$  in Figure 3c (note the inverted direction of the curves in Figure 3c as compared to Figure 3b). Next, we insert

$$f(\omega) = -\frac{1}{\beta\hbar} \frac{d}{d\omega} \ln(1 + e^{-\beta\hbar\omega}) \quad (28)$$

and integrate by parts. Thereby the Fermi function and the factor  $e^{\eta\omega}$  again make sure that the contributions from  $\text{Re}(\omega) = \pm\infty$  vanish and we obtain

$$\begin{aligned} & \frac{1}{\beta} \frac{1}{2\pi i} \oint_{\mathcal{C}'} d\omega \ln(1 + e^{-\beta\hbar\omega}) \frac{d}{d\omega} \left( e^{\eta\omega} \sum_{n=1}^{2n_{orb}} \ln(-\omega + (\mu - E_n(\mathbf{k}))/\hbar) \right) \\ &= \frac{1}{\beta} \frac{1}{2\pi i} \oint_{\mathcal{C}'} d\omega \ln(1 + e^{-\beta\hbar\omega}) e^{\eta\omega} \sum_{n=1}^{2n_{orb}} \frac{\hbar}{\hbar\omega + \mu - E_n(\mathbf{k})} + \mathcal{O}(\eta). \end{aligned}$$

Now we substitute  $\hbar\omega \rightarrow z$  and use the theorem of residues (remembering that  $\mathcal{C}'$  encircles the poles of the Green function on the real axis in *clockwise* fashion) and after taking the limit  $\eta \rightarrow 0$  obtain the expression (24), which completes the first step of the proof.

### 3.3 Calculation of $\partial\Omega/\partial\lambda$

To obtain the derivative of the true grand potential  $\Omega$  with respect to  $\lambda$  we start from the formula

$$\begin{aligned} \lambda \frac{\partial}{\partial\lambda} \Omega(\lambda) &= -\frac{1}{\beta} \lambda \frac{\partial}{\partial\lambda} \ln(\text{Tr}(e^{-\beta(H_0 + \lambda H_1) - \mu N})) \\ &= \frac{1}{Z} \text{Tr}(\lambda H_1 e^{-\beta(H_0 + \lambda H_1) - \mu N}) = \langle \lambda H_1 \rangle_\lambda \end{aligned}$$

where  $\langle \dots \rangle_\lambda$  denotes the thermal average *calculated at interaction strength*  $\lambda$ . The last quantity thus is the expectation value of the interaction Hamiltonian for interaction strength  $\lambda$ . It can be

computed by making use of the equation of motion of the Green function which is a procedure found in many textbooks, see e.g. Equation (23.14) of FW. One has

$$\langle \lambda H_1 \rangle_\lambda = -\frac{1}{2} \lim_{\tau \rightarrow 0^-} \sum_{\mathbf{k}} \text{Tr} \left( \hbar \frac{\partial}{\partial \tau} - \mu + \mathbf{t}(\mathbf{k}) \right) \mathbf{G}_\lambda(\mathbf{k}, \tau),$$

where the subscript  $\lambda$  on the Green function implies that this is the exact Green function for interaction strength  $\lambda$ . Next we recall the Dyson equation (16), which holds for any  $\lambda$

$$\left( -\partial_\tau + \frac{\mu}{\hbar} - \frac{1}{\hbar} \mathbf{t}(\mathbf{k}) \right) \mathbf{G}(\mathbf{k}, \tau) - \int_0^{\beta\hbar} \Sigma(\mathbf{k}, \tau - \tau') \mathbf{G}(\mathbf{k}, \tau') d\tau' = \delta(\tau).$$

Since  $\delta(\tau < 0) = 0$  we have  $\lim_{\tau \rightarrow 0^-} \delta(\tau) = 0$  and obtain

$$\begin{aligned} \lambda \frac{\partial}{\partial \lambda} \Omega(\lambda) &= \frac{\hbar}{2} \lim_{\tau \rightarrow 0^-} \sum_{\mathbf{k}} \int_0^{\beta\hbar} d\tau' \text{Tr} \left( \Sigma_\lambda(\mathbf{k}, \tau - \tau') \mathbf{G}_\lambda(\mathbf{k}, \tau') \right) \\ &= \frac{1}{2\beta} \sum_{\mathbf{k}, \nu} \text{Tr} \Sigma_\lambda(\mathbf{k}, i\omega_\nu) \mathbf{G}_\lambda(\mathbf{k}, i\omega_\nu). \end{aligned} \quad (29)$$

### 3.4 Definition and properties of the Luttinger-Ward functional

As already mentioned  $\Phi[\mathbf{G}]$  is defined as a sum over infinitely many Feynman diagrams with certain properties. The diagrams which contribute are *closed*, which means they have no external lines. They are moreover *connected*, which means that they cannot be decomposed into sub-diagrams which are not connected by lines. And finally, only *skeleton diagrams* are taken into account in the Luttinger-Ward functional. A skeleton diagram is a diagram where no Green function line contains a self-energy insertion. In other words, it is impossible to draw a box around any part of the diagram, so that only two Green function lines cross the box.

At this point we need to discuss an important property of the skeleton diagrams. Let us consider a self-energy diagram. It contains one Green function line from the entry-point to the exit-point, and a number of Green function loops. Starting from the entry-point we may follow the Green function line and draw a circle around each self-energy insertion that we encounter until we reach the exit point. This procedure will eliminate a number of loops, that means enclose them in a self-energy insertion. Then, we continue along the first interaction line which is not eliminated until we reach a Fermion loop that is not yet eliminated. We follow the Green function line along this loop and again draw a circle around each self-energy insertion. We proceed to the next interaction line that has not yet been eliminated and so on. We end up with a diagram in which all self-energy insertions are inside circles. Replacing the circles by straight lines, we obviously obtain a skeleton-diagram for the self-energy. It is easy to see that the skeleton diagram to which a given self-energy diagram is reduced is unique. All self-energy diagrams thus can be grouped into classes such that all members of one class can be reduced to the same skeleton diagram. Conversely, all members of one class can be obtained by starting out from the skeleton-diagram and inserting the full Green function for each Green function line in the

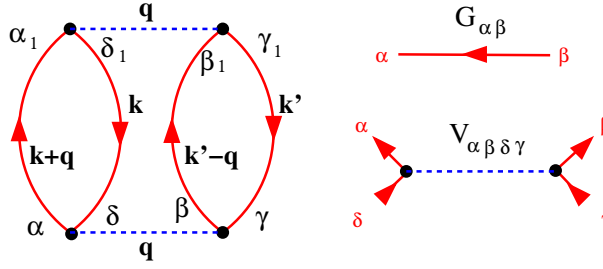


**Fig. 4:** Left: A diagram contributing to the Luttinger-Ward functional. Right: the elements of the diagram.

diagram, which we write as

$$\Sigma(\mathbf{k}, \omega) = \sum_n \Sigma^{(s,n)}(\mathbf{k}, \omega). \quad (30)$$

Here  $\Sigma^{(s,n)}$  denotes the set of all  $n^{\text{th}}$  order skeleton diagrams (i.e. diagrams with  $n$  interaction lines) with the Green function lines replaced by the full Green function.

Having defined the diagrams contributing to  $\Phi[\mathbf{G}]$  each diagram is now translated into a multiple sum according to the standard Feynman rules for the imaginary-time Green function in momentum space (see section 25 of FW). However, there is one crucial difference: whereas in a standard Feynman diagram a Green function line corresponds to a factor  $\mathbf{G}^0(\mathbf{k}, \omega)$  (the non-interacting Green function), in the Luttinger-Ward functional we replace  $\mathbf{G}^0(\mathbf{k}, \omega) \rightarrow \mathbf{G}(\mathbf{k}, \omega)$  where  $\mathbf{G}(\mathbf{k}, \omega)$  is the argument of the functional  $\Phi[\mathbf{G}]$ . As an example, the expression corresponding to the diagram in Figure (4) is

$$\left(\frac{-1}{\beta\hbar^2 N}\right)^2 (-1)^2 \sum_{\mathbf{k}, \mathbf{k}', \mathbf{q}} \sum_{\alpha, \beta, \gamma, \delta} \sum_{\alpha_1, \beta_1, \gamma_1, \delta_1} \sum_{\nu, \nu', \mu} V_{\alpha, \beta, \delta, \gamma}(\mathbf{k}, \mathbf{k}', \mathbf{q}) V_{\delta_1, \gamma_1, \alpha_1, \beta_1}(\mathbf{k}+\mathbf{q}, \mathbf{k}'-\mathbf{q}, -\mathbf{q}) \\ \times G_{\alpha_1, \alpha}(\mathbf{k}+\mathbf{q}, i\omega_\nu + \omega_\mu) G_{\delta, \delta_1}(\mathbf{k}, i\omega_\nu) G_{\beta_1, \beta}(\mathbf{k}'-\mathbf{q}, \omega_{\nu'} - \omega_\mu) G_{\gamma, \gamma_1}(\mathbf{k}', \omega_{\nu'}). \quad (31)$$

The Luttinger-Ward functional  $\Phi[\mathbf{G}]$  thus consists of an infinite sum of multiple sums which involve the interaction matrix elements  $V$  of the Hamiltonian (23) and the function  $\mathbf{G}$  for which the functional is to be evaluated.

Let us briefly discuss the scaling with system size,  $N$ . By the Feynman rules an  $n^{\text{th}}$  order diagram has the prefactor  $(1/N)^n$ . On the other hand, there are  $n$  interaction lines, and  $2n$  Green function lines, so that there are  $3n$  momenta. The  $n$  interaction lines give rise to  $2n$  momentum conservation conditions, one for each end of a line. However, in a *closed* diagram one of these momentum conservation conditions is fulfilled trivially so that there remain  $n+1$  momenta to be summed over (see the above example). Each sum runs over  $N$  momenta so that the total diagram is of order  $N$ , as it has to be because  $\Omega$  is an extensive quantity.

In addition to the factors originating from the Feynman rules, each diagram is multiplied by  $-1/(\beta S)$  where the positive integer  $S$  is the *symmetry factor* of the diagram. A very detailed discussion of these symmetry factors is given in section 2.3 of Negele-Orland [7]. The definition is as follows: first, the diagram is drawn such that all interaction lines are in  $x$ -direction. The  $n$  interaction lines of a diagram are labeled by integers  $i \in \{1 \dots n\}$  and the

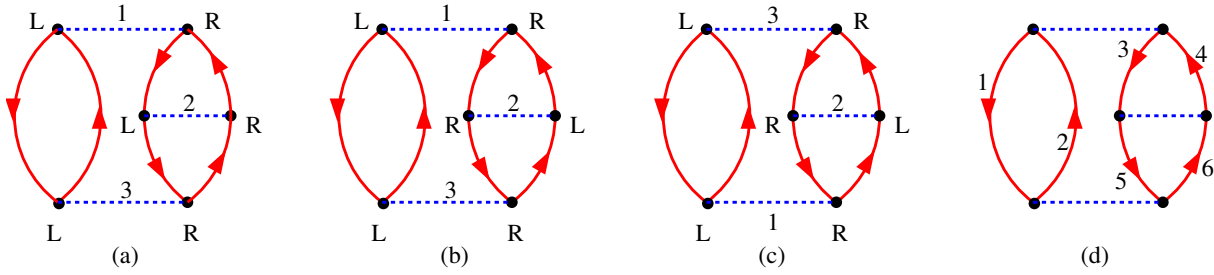


**Fig. 5:** Determination of the symmetry factor  $S$  for a diagram.

ends of each interaction line are labeled by  $R$  and  $L$  (for ‘right end’ and ‘left end’), see Figure 5(a). Any Green function line in the diagram now can be labeled by the ends of the interaction lines where it departs and where it ends:  $(i, S_1) \rightarrow (j, S_2)$  with  $i, j \in \{1 \dots n\}$  and  $S_1, S_2 \in \{R, L\}$ . Obviously, the diagram is characterized completely by the  $2n$  ‘directed quadruples’  $(i, S_1) \rightarrow (j, S_2)$ . Then, we consider the following operations on the diagrams: a) any permutation of the indices  $i$ , b) exchange of the labels  $R$  and  $L$  on an arbitrary number of interaction lines, c) any combination of a permutation followed by label exchanges. Such an operation obviously changes the quadruples which characterize the connectivity of the diagram:  $[(i, S_1) \rightarrow (j, S_2)] \rightarrow [(i', S'_1) \rightarrow (j', S'_2)]$ . The symmetry factor of a diagram then is the number of symmetry operations—including identity—where the new labels  $(i', S'_1) \rightarrow (j', S'_2)$  are a permutation of the old ones,  $(i, S_1) \rightarrow (j, S_2)$  (Negele-Orland then call the transformed diagram a deformation of the first one). As an example, consider the diagram in Figure 5(a). Label exchange on, say, interaction line 2 leads to the diagram shown in 5(b) which, however, is not a deformation of the original diagram. This can be seen by considering, e.g., the line connecting the  $R$ -end of 1 and the  $R$ -end of 2. In 5(a) this line would have the label  $(2, R) \rightarrow (1, R)$ , whereas it would be  $(1, R) \rightarrow (2, R)$  in 5(b). This means that the direction of momentum flow along the line would be reversed. On the other hand, the permutation of the labels 1 and 3 followed by label exchange on interaction line 2 leads to the diagram 5(c) which indeed is a deformation of the original diagram. In Figure 5(d) the Green function lines are numbered by  $1 \rightarrow 6$  and Table 1 gives the quadruples corresponding to these lines in Figures 5(a) and 5(c). Obviously the two sets of quadruples are a permutation of each other.

Line	5(a)	5(c)
1	$(1, L) \rightarrow (3, L)$	$(3, L) \rightarrow (1, L)$
2	$(3, L) \rightarrow (1, L)$	$(1, L) \rightarrow (3, L)$
3	$(1, R) \rightarrow (2, L)$	$(3, R) \rightarrow (2, R)$
4	$(2, R) \rightarrow (1, R)$	$(2, L) \rightarrow (3, R)$
5	$(2, L) \rightarrow (3, R)$	$(2, R) \rightarrow (1, R)$
6	$(3, R) \rightarrow (2, R)$	$(1, R) \rightarrow (2, L)$

**Table 1:** Quadruples describing the connectivity of the diagrams Figure 5a and Figure 5c. The numbers of the Green function lines are given in Figure 5d.

It turns out that this is the only symmetry operation which leaves the diagram invariant, so that, taking into account the identity operation, the diagram has  $S = 2$ . Since a symmetry operation corresponds to a permutation of the quadruples  $(i, S_1) \rightarrow (j, S_2)$  which characterize the individual Green function lines in a diagram it defines a mapping between these lines whereby each line is mapped onto the one which gets its label. For example, from Table 1 one reads off the corresponding mapping for the operation connecting 5a and 5c:

$$\begin{array}{cccccc} 1 & 2 & 3 & 4 & 5 & 6 \\ 2 & 1 & 6 & 5 & 4 & 3 \end{array}$$

If two Green function lines  $i$  and  $j$  are mapped onto each other, the lines are equivalent in the sense that the diagram could be deformed such that the deformed diagram is precisely the same as the original one but line  $j$  now taking the place of line  $i$  and vice versa.

Let us now assume that a diagram has the symmetry factor  $S$ . This means that all Green function lines can be grouped into disjunct classes such that the lines belonging to one class are mapped onto each other by one of the  $S$  symmetry operations. For example, the diagram in 5 has the classes  $(1, 2)$ ,  $(3, 6)$ , and  $(4, 5)$ . Since a diagram with  $n$  interaction lines has  $2n$  Green function lines the number of classes is  $2n/S$  which will be of importance later on.

Next, we want to see the meaning of this definition. In fact, the Luttinger-Ward functional is the *generating functional* of the self-energy, or, more precisely,

$$\frac{\partial \Phi}{\partial G_{\alpha,\beta}(\mathbf{k}, i\omega_\nu)} = \frac{1}{\beta} \Sigma_{\beta,\alpha}(\mathbf{k}, i\omega_\nu). \quad (32)$$

To see this, consider an infinitesimal change  $G_{\alpha\beta}(\mathbf{k}, i\omega_\nu) \rightarrow G_{\alpha\beta}(\mathbf{k}, i\omega_\nu) + \delta G_{\alpha\beta}(\mathbf{k}, i\omega_\nu)$  as in Figure 6. The initial diagrams correspond to multiple sums over products of Green functions where all internal frequencies, momenta, and orbital indices are summed over, subject to the condition of energy/momentum conservation at each interaction vertex, see (31). The first order change then also can be viewed as a sum of diagrams but with a single missing line—this corresponds to the variation  $\delta G$  which has been factored out. Another way to state this is to say that differentiating with respect to an element of  $\mathbf{G}$  amounts to successively ‘open’ each of the lines in the initial closed diagram and sum the remaining diagrams. These remaining diagrams obviously ‘look like’ self-energy diagrams in that they have two entry points. We now need to show, however, that the diagrams not only ‘look like’ possible contributions to the skeleton diagram expansion of the self-energy, but that they come with exactly the right numerical prefactors. At this point, the additional prefactors of  $-1/\beta S$  turn out to be crucial.

We first note that the momentum and frequency which flow into/out of the diagram are fixed by the momentum and frequency of  $\delta G$ . As regards the orbital indices, we recall that  $G_{\alpha\beta}$  corresponds to a directed line  $\beta \rightarrow \alpha$ . The resulting self-energy-like diagrams therefore all have the matrix index  $\alpha$  on their incoming entry and  $\beta$  on their outgoing entry, and comparing with Figure 4 we see that this assignment of indices corresponds to  $\Sigma_{\beta\alpha}$ . Moreover, all internal momenta, frequencies, and matrix indices in the remaining diagrams are summed over—subject to the condition of frequency and momentum conservation at the interaction lines—as would

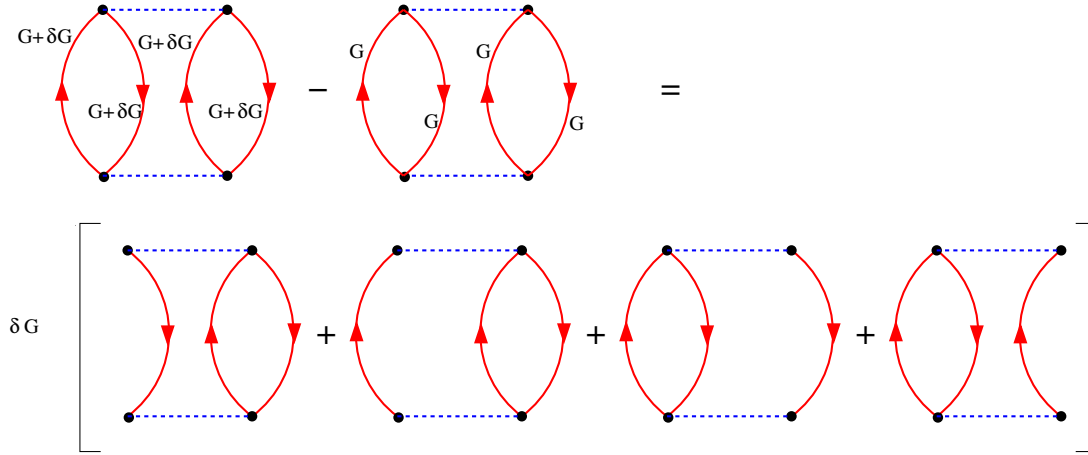


**Fig. 6:** Variation of  $\mathbf{G}$  implies ‘opening’ the lines of a Feynman diagram.

be the case in the true self-energy diagrams. Second, the order  $n$  of a diagram—that means the number of interaction lines—is not changed by opening a Green function line, so that the prefactor  $-1/(\beta\hbar^2 N)^n$  of the closed diagram is also the correct prefactor for the resulting self-energy diagram. Third, opening a Green function line reduces the number of closed Fermion loops by 1 and the factor  $(-1)$  in  $(-\frac{1}{\beta S})$  takes care of this. And, lastly, we need to discuss the symmetry factor  $S$ . Let us consider a diagram with  $n$  interaction lines, which accordingly has  $2n$  Green function lines and moreover assume that the diagram has the symmetry factor  $S$ . As we saw above, the  $2n$  Green function lines can be divided into classes of  $S$  members which are mapped into each other by the symmetry operations and the number of these classes is  $2n/S$ . A symmetry operation maps a Green function line  $i$  onto an equivalent one  $j$ , so that it is possible to deform the diagram such that it looks exactly the same as the original one, but with line  $j$  in place of line  $i$ . This means, however, that ‘opening’ the line  $i$  also gives *exactly* the same self-energy diagram as opening line  $j$ . Accordingly, from the single closed diagram of degree  $n$  with symmetry factor  $S$  we obtain  $2n/S$  different skeleton diagrams for the self-energy, and each is produced  $S$  times, see also Figure 7. This factor of  $S$ , however, precisely cancels the prefactor  $1/S$ . It follows, that each skeleton-diagram for the self-energy is produced with same prefactor  $1/\beta$ . Differentiating  $\Phi[\mathbf{G}]$  with respect to  $G_{\alpha\beta}(\mathbf{k}, i\omega_\nu)$  thus gives  $1/\beta$  times the sum of all skeleton diagrams for  $\Sigma_{\beta\alpha}(\mathbf{k}, i\omega_\nu)$ , with the noninteracting Green function replaced by the full one, and this is exactly  $\Sigma_{\beta\alpha}(\mathbf{k}, i\omega_\nu)$  itself, see (30), so that (32) is proved.

We have just seen, that all skeleton-diagrams for the self-energy can be obtained by differentiating the Luttinger-Ward functional with respect to  $\mathbf{G}$ , whereby the differentiation corresponds to ‘opening’ one line in a closed diagram. We then may ask if this operation can be reversed, namely if the Luttinger-Ward functional can be obtained by starting from the skeleton-diagram expansion of the self-energy and ‘close’ the diagrams by ‘reconnecting’ the entry-points of the self-energy by a Green function. More precisely, we consider

$$\frac{1}{\beta} \sum_{\nu, \mathbf{k}} \sum_{\alpha, \beta} \mathbf{G}_{\alpha, \beta}(\mathbf{k}, i\omega_\nu) \Sigma_{\beta, \alpha}^{(s, n)}(\mathbf{k}, i\omega_\nu). \quad (33)$$



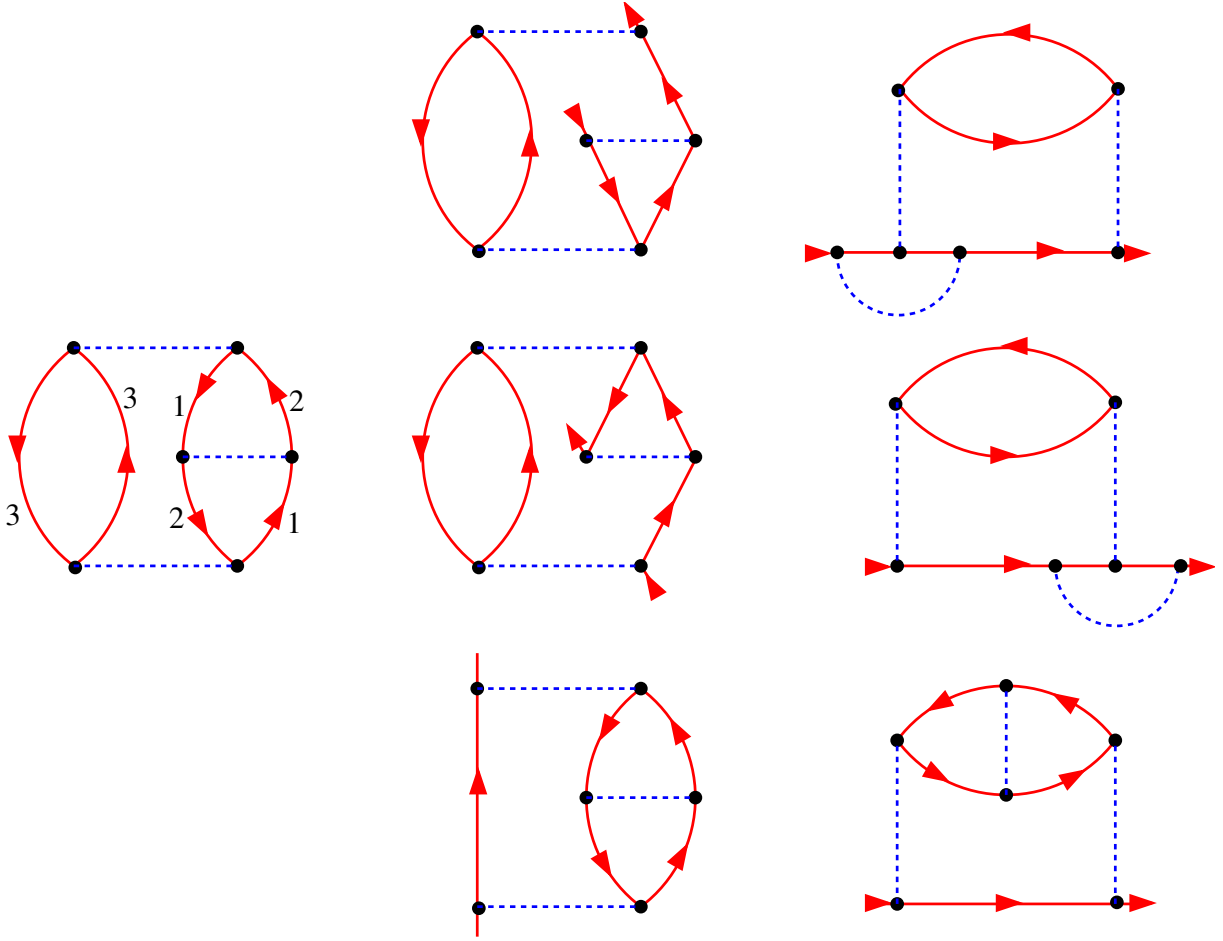


**Fig. 7:** The diagram on the left has  $n = 3$  and  $S = 2$  and accordingly 3 classes of symmetry-equivalent Green function lines. The lines are labeled by the number of the classes, compare Figure 5 and Table 1. Successively opening the lines of the diagram produces the three different self-energy diagrams in the center column and each of them is produced  $S = 2$  times. The right column shows the diagrams redrawn to more look like self-energy diagrams.

We have seen that an  $n^{\text{th}}$  order diagram contributing to  $\Phi[\mathbf{G}]$  with symmetry factor  $S$  produces  $2n/S$  different skeleton-self-energy diagrams, and each of them  $S$  times and with a factor of  $(-1)$ , so that the remaining prefactor was  $1/\beta$ . Upon closing the Fermion line again, according to (33), each of these diagrams produces the original closed diagram (it is easy to see that for each self-energy diagram there is exactly one closed diagram from which it can be obtained). Since there are  $2n/S$  self-energy diagrams originating from the original closed diagram the latter is produced  $2n/S$  times and thus has the additional prefactor  $-2n/S\beta$  (the factor of  $(-1)$  is due to the additional Fermion loop in the closed diagram). In the expansion of  $\Phi[\mathbf{G}]$ , however, the diagram would have had the prefactor  $-1/S\beta$ , or, put another way, closing the sum of all  $n^{\text{th}}$  order skeleton diagrams for  $\Sigma$ , according to (33), produces the  $n^{\text{th}}$  order contribution to  $\Phi[\mathbf{G}]$  with an additional prefactor of  $2n$  so that

$$\Phi^{(n)} = \frac{1}{2n\beta} \sum_{\nu, \mathbf{k}} \text{Tr} \mathbf{G}(\mathbf{k}, i\omega_\nu) \Sigma^{(s,n)}(\mathbf{k}, i\omega_\nu). \quad (34)$$

Lastly, we give one more comment on the symmetry factors. Readers who wish to study the original paper of Luttinger and Ward, which is highly recommended, will realize that no symmetry factors appear in this work. The reason is that LW carry out their derivation using what Negele-Orland (NO) call ‘labeled Feynman diagrams’. For example, LW’s equation (17) corresponds precisely to NO’s equation (2.96). The derivation in the present notes, however, uses what NO call ‘unlabeled Feynman diagrams’. The transition between these two types of diagrams and the emergence of the symmetry factors thereby is discussed in detail in section 2.3 of NO [7].

### 3.5 Calculation of $\partial\tilde{\Omega}/\partial\lambda$

We proceed to the final step of the proof and compute  $\partial\tilde{\Omega}/\partial\lambda$ . If we vary the interaction strength  $\lambda$ , there are two places in the expression for  $\Omega'$ , eqn. (25), where this makes it self felt. Namely the self-energy  $\Sigma$  will change and moreover the interaction matrix elements  $V$  in the Luttinger-Ward functional (see, e.g., eqn. (31)) which have a prefactor of  $\lambda$  will also contribute to the variation. Let us first consider the variation of  $\Sigma$  and compute

$$\frac{\partial\Omega'}{\partial\Sigma_{\alpha,\beta}(\mathbf{k}, i\omega_\nu)}.$$

There are three terms in (25) and we consider them one after the other. The first two terms involve a sum over momentum and frequency and obviously only those terms with momentum  $\mathbf{k}$  and frequency  $\omega_\nu$  will contribute. Accordingly, in the following equations we omit the arguments  $(\mathbf{k}, i\omega_\nu)$  for brevity. Then we find by using the chain rule for differentiation

$$\begin{aligned} \frac{\partial}{\partial\Sigma_{\alpha,\beta}} \left( -\frac{1}{\beta} \ln \det (-\mathbf{G}^{-1}) \right) &= -\frac{1}{\beta} \sum_{\mu,\nu} \left( \frac{\partial}{\partial(-G_{\mu,\nu}^{-1})} \ln \det (-\mathbf{G}^{-1}) \right) \frac{\partial(-G_{\mu,\nu}^{-1})}{\partial\Sigma_{\alpha,\beta}} \\ &= -\frac{1}{\beta} \sum_{\mu,\nu} (-G_{\nu,\mu}) \delta_{\mu,\alpha} \delta_{\nu,\beta} \\ &= \frac{1}{\beta} G_{\beta,\alpha}. \end{aligned}$$

In going to the 2<sup>nd</sup> line we used the identity from Appendix B and the Dyson equation

$$-\mathbf{G}^{-1} = -\omega - \mu + \Sigma$$

from which it follows that

$$\frac{\partial(-G_{\mu,\nu}^{-1})}{\partial\Sigma_{\alpha,\beta}} = \delta_{\mu,\alpha} \delta_{\nu,\beta}.$$

We proceed to the second term,

$$\frac{\partial}{\partial\Sigma_{\alpha,\beta}} \left( -\frac{1}{\beta} \text{Tr} \Sigma \mathbf{G} \right) = \frac{\partial}{\partial\Sigma_{\alpha,\beta}} \left( -\frac{1}{\beta} \sum_{\mu,\nu} \Sigma_{\nu,\mu} G_{\mu,\nu} \right) = -\frac{1}{\beta} \left( G_{\beta,\alpha} + \sum_{\mu,\nu} \Sigma_{\nu,\mu} \frac{\partial G_{\mu,\nu}}{\partial\Sigma_{\alpha,\beta}} \right).$$

Lastly we consider the Luttinger-Ward functional. Using again the chain rule we find

$$\frac{\partial \Phi[G]}{\partial \Sigma_{\alpha,\beta}} = \sum_{\mu,\nu} \frac{\partial \Phi[G]}{\partial G_{\mu,\nu}} \frac{\partial G_{\mu,\nu}}{\partial \Sigma_{\alpha,\beta}} = \frac{1}{\beta} \sum_{\mu,\nu} \Sigma_{\nu,\mu} \frac{\partial G_{\mu,\nu}}{\partial \Sigma_{\alpha,\beta}}.$$

Adding up the three terms we thus obtain the important result

$$\frac{\partial \Omega'}{\partial \Sigma_{\alpha,\beta}(\mathbf{k}, i\omega_\nu)} = 0. \quad (35)$$

In other words: the expression  $\Omega'$ , which will be seen to be equal to the grand potential  $\Omega$  in a moment, is stationary with respect to variations of the self-energy! This is the stationarity condition for  $\Sigma$  which is the basis of the VCA.

First, however, we have to complete the proof and evaluate  $\lambda \frac{\partial}{\partial \lambda} \Omega'(\lambda)$ . Since there is no variation of  $\Omega'$  due to a variation of  $\Sigma$ , the only remaining source of variation are the interaction lines in the Luttinger-Ward functional. Namely any  $n^{\text{th}}$  order diagram has the prefactor of  $\lambda^n$  so that

$$\lambda \frac{\partial}{\partial \lambda} \Phi^{(n)} = n \Phi^{(n)}$$

Using (34) we thus obtain

$$\begin{aligned} \lambda \frac{d\Omega'}{d\lambda} &= \sum_n n \Phi^{(n)} = \sum_n \frac{1}{2\beta} \sum_{\nu,\mathbf{k}} \text{Tr} \mathbf{G}_\lambda(\mathbf{k}, i\omega_\nu) \Sigma_\lambda^{(s,n)}(\mathbf{k}, i\omega_\nu) \\ &= \frac{1}{2\beta} \sum_{\nu,\mathbf{k}} \text{Tr} \mathbf{G}_\lambda(\mathbf{k}, i\omega_\nu) \left( \sum_n \Sigma_\lambda^{(s,n)}(\mathbf{k}, i\omega_\nu) \right) \\ &= \frac{1}{2\beta} \sum_{\nu,\mathbf{k}} \text{Tr} \mathbf{G}_\lambda(\mathbf{k}, i\omega_\nu) \Sigma_\lambda(\mathbf{k}, i\omega_\nu). \end{aligned}$$

Comparing with (29) we see that this is equal to  $\lambda \frac{\partial}{\partial \lambda} \Omega(\lambda)$  which completes the proof.

Let us summarize the results which we have obtained:

1. The grand canonical potential  $\Omega$  of an interacting Fermi system is given by (25).
2. The Luttinger-Ward functional is the generating functional of  $\Sigma(\mathbf{k}, i\omega_\nu)$ , see eqn. (32).
3. The Luttinger-Ward functional depends only on the interaction matrix elements  $V_{\alpha\beta\delta\gamma}$  in the Hamiltonian and the Green function  $\mathbf{G}$  which is the argument of the functional.
4.  $\Omega$  is stationary under variations of  $\Sigma(\mathbf{k}, i\omega_\nu)$  see (35).

Looking at the above proof one might worry about the fact that it assumes a continuous evolution of the system with increasing interaction strength  $\lambda$ , whereas we are also interested, e.g., in Mott-insulators where we have reason to believe that a phase transition occurs as a function of  $\lambda$ . However, Potthoff has recently given a nonperturbative proof of the theorem [12, 11] that means all of the above properties of the grand potential, the Luttinger-Ward functional and the self-energy remain valid in a strongly correlated electron system where a Feynman-diagram expansion of the Green function and the adiabatic continuity with the noninteracting system can no longer be assumed valid.

## 4 Conserving approximations

An important application of the Luttinger-Ward functional is the construction of conserving approximations. To discuss these, we will use a special form of the Hamiltonian for the remainder of this section. We assume that the set of quantum numbers reduces to  $\alpha = \mathbf{r}$  that means we neglect spin for simplicity. To follow the notation common in the literature we denote the electron creation operator by  $\Psi^\dagger(\mathbf{r})$  instead of  $a_\alpha^\dagger$ . The Hamiltonian for a homogeneous system is

$$H = \frac{\hbar^2}{2m} \int d\mathbf{r} \nabla \Psi^\dagger(\mathbf{r}) \cdot \nabla \Psi(\mathbf{r}) + \frac{1}{2} \int d\mathbf{r} \int d\mathbf{r}' \Psi^\dagger(\mathbf{r}) \Psi^\dagger(\mathbf{r}') V(\mathbf{r}-\mathbf{r}') \Psi(\mathbf{r}') \Psi(\mathbf{r}).$$

We assume that we can always perform a partial integration and drop the surface terms. In this way the first term in  $H$  can be brought to either of the two forms  $-\frac{\hbar^2}{2m} \int d\mathbf{r} \Psi^\dagger(\mathbf{r})(\nabla^2 \Psi(\mathbf{r}))$  or  $-\frac{\hbar^2}{2m} \int d\mathbf{r} (\nabla^2 \Psi^\dagger(\mathbf{r})) \Psi(\mathbf{r})$ . Since the system is homogeneous the electron density is  $n_0$ , independent of position. We now assume that the system is acted upon by a perturbation of the form  $H_p = \int d\mathbf{r} U(\mathbf{r}, t) n(\mathbf{r})$ , i.e., a time dependent real potential  $U$  which couples to the electron density  $n(\mathbf{r}) = \Psi^\dagger(\mathbf{r}) \Psi(\mathbf{r})$ . Thereby we demand that  $\int d\mathbf{r} U(\mathbf{r}, t) = 0$  for all  $t$  because a constant component would merely shift the zero of energy and not induce any response. As we have seen—or rather: quoted from FW—in the first section, the change of the expectation value of any operator  $A(\mathbf{r})$  to first order in  $U$  is given by

$$\begin{aligned} \delta \langle A(\mathbf{r}) \rangle(t) &= \frac{1}{\hbar} \int d\mathbf{r}' \int_{-\infty}^{\infty} dt' G_{A,n}^R(\mathbf{r}t, \mathbf{r}'t') U(\mathbf{r}', t'), \\ G_{A,n}^R(\mathbf{r}t, \mathbf{r}'t') &= -i\Theta(t-t') \langle [A(\mathbf{r}, t), n(\mathbf{r}', t')] \rangle_{th}. \end{aligned}$$

Now we may choose  $A(\mathbf{r})$  to be the operator  $n(\mathbf{r})$  of electron density or the operator of electron current  $\mathbf{j}(\mathbf{r}) = \frac{i\hbar}{2m} ((\nabla \Psi^\dagger(\mathbf{r})) \Psi(\mathbf{r}) - \Psi^\dagger(\mathbf{r}) \nabla \Psi(\mathbf{r}))$ . Assuming that in the unperturbed state of the system there is no current and that the electron density is time independent, the induced changes must fulfill certain conservation laws:

$$\begin{aligned} \frac{\partial \delta n(\mathbf{r})}{\partial t} + \nabla \cdot \delta \mathbf{j}(\mathbf{r}) &= 0, \\ \frac{d}{dt} \int d\mathbf{r} m \delta \mathbf{j}(\mathbf{r}) &= \int d\mathbf{r} \left( -\nabla U(\mathbf{r}, t) \right) \delta n(\mathbf{r}, t) \\ \frac{d}{dt} \langle H \rangle &= \int d\mathbf{r} \left( -\nabla U(\mathbf{r}, t) \right) \cdot \delta \mathbf{j}(\mathbf{r}) \end{aligned}$$

The first line is the continuity equation, the second line states that the total momentum of the electron system changes according to Newton's law and the third equation states that the change of the total energy of the system is equal to the work done by the external force (in the second equation we have used that by partial integration the right hand side can be converted to  $\int d\mathbf{r} U(\mathbf{r})(\nabla n(\mathbf{r}))$  so that the constant component of  $n$  does not contribute). Since in general we have to make some approximation to compute the retarded Green function, however, it is not a priori clear that these equations are fulfilled. The imaginary time Green functions  $G_{n,n}$  and

$G_{j,n}$  can be expressed as limits of the two-particle Green function  $G_2$  and the self-energy also is related to  $G_2$ , so that approximating  $\Sigma$  by a functional of the Green function gives us also an approximation for the response function. Building on the work of Luttinger and Ward, Baym has given a prescription to construct approximations for  $\Sigma$  which guarantee that the resulting response functions obey all conservation laws and we want to outline his ideas. To simplify the notation we introduce the ‘compound coordinate’  $x = (\mathbf{r}\tau)$  and it is understood that operators such as  $n(x)$  which have  $x$  as an argument are imaginary-time Heisenberg operators. Moreover we denote

$$\int dx \cdots = \int_0^{\beta\hbar} d\tau \int d\mathbf{r} \cdots$$

We first generalize the definition of the imaginary-time single particle Green function

$$\begin{aligned} G(x, x')[U] &= -\frac{1}{Z[U]} \left\langle T \left[ \Psi(x) \Psi^\dagger(x') \exp \left\{ \frac{1}{\hbar} \int dx_1 U(x_1) n(x_1) \right\} \right] \right\rangle_{th}, \\ Z[U] &= \left\langle T \left[ \exp \left\{ \frac{1}{\hbar} \int dx_1 U(x_1) n(x_1) \right\} \right] \right\rangle_{th}. \end{aligned} \quad (36)$$

This modified Green function is a functional of the real and time dependent potential  $U(x)$  and depends on  $\tau$  and  $\tau'$  separately. It is obvious that as  $U \rightarrow 0$  it reduces to the ordinary Green function discussed so far. Moreover, using the cyclic property of the trace it can again be shown that this Green function obeys the same boundary condition  $G(\beta\hbar) = -G(0)$  as the ordinary Green functions and thus has a Fourier expansion of the type (6). It should be stressed, that this Green function is defined for imaginary times and has no direct physical interpretation.

We now consider the functional derivative of  $G$  with respect to  $U(x_1)$ . This is defined as the change of  $G[U]$  under an infinitesimal ‘ $\delta$ -spike’,  $U(x) \rightarrow U(x) + \epsilon\delta(x-x_1)$ . One may also think of the integrals in (36) as the limit of sums over grid points  $x_i$ , the functional derivative then is the limit of the derivative with respect to the value of  $U$  at the grid point closest to  $x_1$ . Using the fact that in the argument of the time-ordering operator  $T$  the operators  $H$  or  $n$  can be commuted with each other and with both,  $\Psi$  and  $\Psi^\dagger$ , one finds

$$\hbar \frac{\delta G(x, x')[U]}{\delta U(x_1)} \Big|_{U=0} = -\langle T[\Psi(x) \Psi^\dagger(x') n(x_1)] \rangle_{th} + G(x, x') n_0.$$

Taking now the limit  $x' \rightarrow x^+ = \mathbf{r}\tau^+$  we find

$$\begin{aligned} \lim_{x' \rightarrow x^+} \hbar \frac{\delta G(x, x')[U]}{\delta U(x_1)} \Big|_{U=0} &= -\langle T[n(x)n(x_1)] \rangle_{th} + n_0^2, \\ \lim_{x' \rightarrow x^+} \hbar \frac{i\hbar}{2m} (\nabla' - \nabla) \frac{\delta G(x, x')[U]}{\delta U(x_1)} \Big|_{U=0} &= -\langle T[\mathbf{j}(x)n(x_1)] \rangle_{th} + \langle \mathbf{j}(x) \rangle_{th} n_0. \end{aligned}$$

It should be noted that for  $U = 0$  we have  $\langle \mathbf{j}(x) \rangle_{th} = 0$  so that the second term in the second equation could have been omitted. The extra terms involving  $n_0$  can be absorbed by re-defining  $n(x) \rightarrow n(x) - n_0$ , i.e., the operator of density fluctuations. We will assume that this has been

done from now on. The above shows that the time-ordered Green function of the operators  $A = n(\mathbf{r})$  or  $A = \mathbf{j}(\mathbf{r})$  and  $B = n(\mathbf{r}_1)$  (which gives us the physical response function when continued analytically to above the real axis) can be obtained by functional differentiation of the modified Green function (36). In fact the only requirement is that  $A$  be quadratic in the field operators or its derivatives, moreover  $n(\mathbf{r})$  can be replaced by any other operator. On the other hand, the Green function involves the self-energy  $\Sigma$ , which we assume to be approximated as a functional of the Green function itself:  $\Sigma = \Sigma[G]$ . The functional derivative—and hence the response functions—therefore depend on the form of  $\Sigma[G]$ . The question then is if it is possible to choose the functional  $\Sigma = \Sigma[G]$  such, that the resulting response functions obey the conservation laws. Baym has shown that the answer to this question is affirmative and in fact the general prescription is to define an approximate Luttinger-Ward functional, which contains only a subset of all possible diagrams and to then construct  $\Sigma$  according to (32):

$$\Sigma_{\alpha,\beta}[G] = \frac{1}{K_B T} \frac{\delta\Phi[G]}{\delta G_{\beta,\alpha}} \Rightarrow \delta\Phi[G] = k_B T \sum_{\alpha,\beta} \Sigma_{\alpha,\beta}[G] \delta G_{\beta,\alpha}. \quad (37)$$

We show that a self-energy constructed in this way obeys the continuity equation: The equation of motion obeyed by the modified Green function is (we suppress the  $[U]$  on all quantities)

$$\left(-\hbar \frac{\partial}{\partial \tau} + \frac{\hbar^2 \nabla^2}{2m} + \mu + U(\mathbf{r}, \tau)\right) G(\mathbf{r}\tau, \mathbf{r}'\tau') = \hbar \delta(\mathbf{r}-\mathbf{r}') \delta(\tau-\tau') \quad (38)$$

$$+ \int d\mathbf{r}_1 V(\mathbf{r}-\mathbf{r}_1) G_2(\mathbf{r}\tau, \mathbf{r}_1\tau, \mathbf{r}'\tau', \mathbf{r}_1\tau').$$

Here the modified  $G_2$  in the presence of  $U$  is defined in a completely analogous way as  $G$ , see (36). We now assume that  $G_2$  is approximated as a functional of  $G$  and replace the approximate  $G_2$  by an approximate  $\Sigma$ . Equation (38) then becomes

$$\left(-\hbar \frac{\partial}{\partial \tau} + \frac{\hbar^2 \nabla^2}{2m} + \mu + U(x)\right) G(x, x') = \hbar \delta(x-x') + \hbar \int dx_1 \Sigma(x, x_1) G(x_1, x'). \quad (39)$$

Next we form  $\int dx \int dx' G(x_2, x) \cdots G^{-1}(x', x_3)$  where  $\cdots$  stands for either the right or left side of (39). We use partial integration to convert, e.g.

$$\int dx G(x_2, x) \left(-\hbar \partial_\tau + \frac{\hbar^2 \nabla^2}{2m}\right) G(x, x') = \int dx \left[ \left(+\hbar \partial_\tau + \frac{\hbar^2 \nabla^2}{2m}\right) G(x_2, x) \right] G(x, x')$$

(here the property  $G(\beta\hbar) = -G(0)$  of the modified Green function is essential!) and exchange  $x_2 \rightarrow x$  and  $x_3 \rightarrow x'$  in the resulting equation. In this way we obtain

$$\left(+\hbar \frac{\partial}{\partial \tau'} + \frac{\hbar^2 \nabla'^2}{2m} + \mu + U(x')\right) G(x, x') = \hbar \delta(x-x') + \hbar \int dx_1 G(x, x_1) \Sigma(x_1, x'). \quad (40)$$

Now we consider the change (with a real function  $\Gamma(x)$ )

$$G(x, x')[U] \rightarrow e^{i\Gamma(x)} G(x, x')[U] e^{-i\Gamma(x')}.$$

In other words, if we represent the Green function  $G(x, x')[U]$  by a directed line from  $x' \rightarrow x$  it is multiplied by  $e^{-i\Gamma(x')}$  for the initial point and by  $e^{i\Gamma(x)}$  for the endpoint. In a closed diagram, however, there is one incoming and one outgoing Green function line at every end of an interaction line  $V(x-x')$  so that the two factors cancel and the value of the diagram remains unchanged whence  $\delta\Phi = 0$ . The crucial point is, that this holds true for each closed diagram individually, so that  $\delta\Phi = 0$  remains true also for an approximate Luttinger-Ward functional in which only a subset of diagrams is kept. On the other hand, if we switch to an infinitesimal  $\Gamma$  we have  $\delta\Phi = \Sigma\delta G$  and for infinitesimal  $\Gamma$  we have  $\delta G(x, x')[U] = i(\Gamma(x) - \Gamma(x')) G(x, x')[U]$ . It follows that (with  $[U]$  again omitted)

$$\Sigma \delta G = i \int dx dx_1 (\Gamma(x_1) - \Gamma(x)) \Sigma(x, x_1) G(x_1, x) = 0.$$

We now interchange integration variables  $x \leftrightarrow x_1$  in the term containing  $\Gamma(x_1)$  and find

$$\int dx dx_1 \Gamma(x) (\Sigma(x, x_1) G(x_1, x) - \Sigma(x_1, x) G(x, x_1)) = 0$$

Since  $\Gamma(x)$  is infinitesimal but arbitrary the  $x_1$  integral must vanish:

$$\int dx_1 (\Sigma(x, x_1) G(x_1, x) - G(x, x_1) \Sigma(x_1, x)) = 0$$

We now subtract (39) from (40), let again  $x' \rightarrow x^+$ :

$$\lim_{x' \rightarrow x^+} \left\{ \left( \hbar \frac{\partial}{\partial \tau} + \hbar \frac{\partial}{\partial \tau'} \right) G(x, x')[U] + \frac{\hbar^2}{2m} (\nabla'^2 - \nabla^2) G(x, x')[U] \right\} = 0,$$

or, using  $\nabla'^2 - \nabla^2 = (\nabla' + \nabla)(\nabla' - \nabla)$

$$\frac{\partial}{\partial \tau} G(x, x^+)[U] - i\nabla \cdot \left[ \lim_{x' \rightarrow x^+} \frac{i\hbar}{2m} (\nabla' - \nabla) G(x, x')[U] \right] = 0.$$

Since  $G(x, x^+) = n(x)$  is the electron density, and the expression in square brackets is the current density at  $\mathbf{j}(x)$ , the Green function obeys a kind of continuity equation. Now we take the functional derivative of both sides with respect to  $U(x')$  and let  $U \rightarrow 0$ . This generates a relation between time-ordered Green functions:

$$\frac{\partial}{\partial \tau} G_{n,n}(\mathbf{r}\tau, \mathbf{r}'\tau') = i\nabla \cdot G_{\mathbf{j},n}(\mathbf{r}\tau, \mathbf{r}'\tau') \Rightarrow i\omega_\nu G_{n,n}(\mathbf{k}, i\omega_\nu) = \mathbf{k} \cdot G_{\mathbf{j},n}(\mathbf{k}, i\omega_\nu),$$

and after performing the analytic continuation  $i\omega_\nu \rightarrow \omega + i\epsilon^+$  we obtain a relation between the physical response functions

$$i\omega G_{n,n}^{(R)}(\mathbf{k}, \omega) - i\mathbf{k} \cdot G_{\mathbf{j},n}^{(R)}(\mathbf{k}, \omega) = 0 \Rightarrow \frac{\partial}{\partial t} G_{n,n}^{(R)}(\mathbf{r}, t) + \nabla \cdot G_{\mathbf{j},n}^{(R)}(\mathbf{r}, t) = 0.$$

The last relation between the response functions, however, does guarantee the validity of the continuity equation for the fluctuations generated by an arbitrary perturbing potential.

Baym and Kadanaoff [3] have investigated under which conditions the momentum conservation

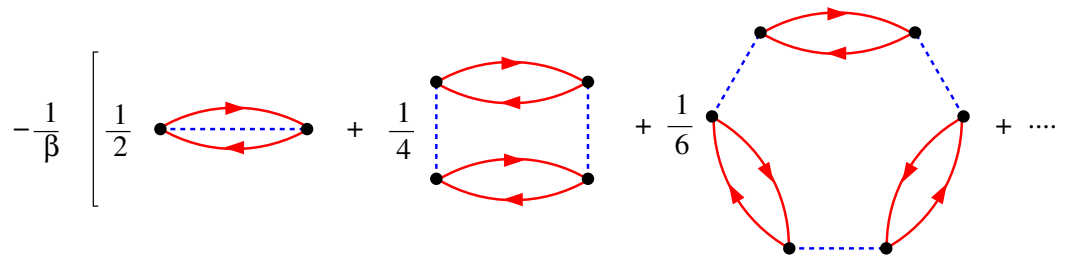


**Fig. 8:** *Approximate Luttinger-Ward functional for the GW approximation.*

law and the energy conservation law are obeyed as well, and Baym [4] has shown that this is always true for a self-energy derived from an approximate Luttinger-Ward functional according to (37). These derivations are more involved, however, so we do not present them here. A famous example of a conserving approximation is the GW-approximation [13]. This can be derived from an approximate Luttinger-Ward functional which contains only ‘bubble-diagrams,’ see Figure 8. As discussed by Negele-Orland, the symmetry factor of a bubble-diagram with  $n$  bubbles is  $2n$ , which explains the prefactors. Another famous conserving approximation is the fluctuation-exchange approximation (or FLEX) [14], which uses a Luttinger-Ward functional comprising bubbles and ladders and has been frequently applied to the Hubbard model.

## 5 Conclusion

To summarize, Luttinger and Ward found an expression for the grand canonical potential of interacting Fermi systems, whereby a key step was the introduction of the Luttinger-Ward functional. This turned out to have additional significance in that it allows the construction of conserving approximations. One issue that we did not touch upon in these notes is the relation to cluster methods which are widely used today. Potthoff has shown [12] that a wide variety of these cluster methods, such as Dynamical Mean-Field Theory or the Dynamical Cluster Approximation can be derived by making use of the stationarity of  $\Omega$  under variation of  $\Sigma$ , equation (35). All of this shows that the Luttinger-Ward functional is a concept of central importance in many-body theory.



## A A theorem on Fourier transforms

Let  $f(t)$  be some function and  $f(\omega)$  its Fourier transform. Then the Fourier transform of the function  $g(t) = -i\Theta(\pm t)f(t)$  is

$$g(\omega) = \pm \frac{1}{2\pi} \int_{-\infty}^{\infty} d\omega' \frac{f(\omega')}{\omega - \omega' \pm i0^+}.$$

To see this we Fourier back-transform  $g(\omega)$ :

$$\frac{1}{2\pi} \int_{-\infty}^{\infty} d\omega e^{-i\omega t} g(\omega) = \pm \frac{1}{4\pi^2} \int_{-\infty}^{\infty} d\omega e^{-i\omega t} \int_{-\infty}^{\infty} d\omega' \frac{f(\omega')}{\omega - \omega' \pm i0^+} \quad (41)$$

We first perform the integral over  $\omega$  and use the trick of closing the integration path by an infinitely large semicircle and use the theorem of residues. We denote  $\omega = \omega_1 + i\omega_2$  so that  $e^{-i\omega t} = e^{\omega_2 t} e^{-i\omega_1 t}$ . For  $t > 0$  ( $t < 0$ ) we therefore have to close in the lower (upper) half-plane to guarantee that the semicircle gives no contribution to the integral. Let us for simplicity consider the upper sign in (41). Then, as a function of  $\omega$  the integrand has a pole at  $\omega = \omega' - i0^+$  and if we close in the upper half-plane, the integration path does not enclose this pole so that the  $\omega$ -integral vanishes. This happens for  $t < 0$  so that the result will be proportional to  $\Theta(t)$ . If we close along the lower half-plane the integration path encloses the pole in clock-wise fashion so we get  $-2\pi i$  times the residue:

$$-i\Theta(t) \frac{1}{2\pi} \int_{-\infty}^{\infty} d\omega' e^{-i\omega' t} f(\omega') = -i\Theta(t)f(t),$$

which proves the theorem.

## B A theorem on determinants

Here we prove the identity

$$\frac{\partial \ln(\det A)}{\partial A_{ij}} = A_{ji}^{-1}.$$

We use Laplace's formula and expand  $\det(A)$  in terms of minors

$$\det(A) = \sum_{l=1, n} (-1)^{i+l} A_{il} M_{il}.$$

Since none of the minors  $M_{il}$  contains the element  $A_{ij}$ , we find

$$\frac{\partial \ln(\det A)}{\partial A_{ij}} = \frac{(-1)^{i+j} M_{ij}}{\det(A)}$$

Next, the  $i^{\text{th}}$  column of  $A^{-1}$  is the solution of the equation system

$$Ac = e_i$$

where  $e_i$  is the  $i^{\text{th}}$  column of the unit matrix. This has all elements equal to zero, except for the  $i^{\text{th}}$ , which is one. We use Cramer's rule and find for the  $j^{\text{th}}$  element of the  $i^{\text{th}}$  column

$$A_{ji}^{-1} = \frac{\det(\bar{A}_j)}{\det(A)},$$

where  $\bar{A}_j$  is the matrix where the  $j^{\text{th}}$  column has been replaced by  $e_i$ . Now we use again Laplace's formula for  $\det(\bar{A}_j)$  and obtain

$$A_{ji}^{-1} = \frac{(-1)^{i+j} M_{ij}}{\det(A)}$$

which proves the theorem.

As an application we assume that the matrix elements of  $A$  are functions of some parameter  $\alpha$ .

Then we find

$$\frac{\partial \ln(\det A)}{\partial \alpha} = \sum_{i,j} \frac{\partial \ln(\det A)}{\partial A_{ij}} \frac{\partial A_{ij}}{\partial \alpha} = \sum_{i,j} A_{ji}^{-1} \frac{\partial A_{ij}}{\partial \alpha} = \text{Tr} \left( A^{-1} \frac{\partial A}{\partial \alpha} \right).$$

## References

- [1] J.M. Luttinger and J.C. Ward, Phys. Rev. **118**, 1417 (1960)
- [2] J.M. Luttinger, Phys. Rev. **119**, 1153 (1960)
- [3] G. Baym and L.P. Kadanoff, Phys. Rev. **124**, 287 (1961)
- [4] G. Baym, Phys. Rev. **127**, 1391 (1962)
- [5] A.A. Abrikosov, L.P. Gorkov and I.E. Dzyaloshinski: *Methods of Quantum Field Theory in Statistical Physics* (Prentice-Hall, New Jersey 1964)
- [6] A.L. Fetter and J.D. Walecka, *Quantum Theory of Many-Particle Systems* (McGraw-Hill, San Francisco, 1971)
- [7] J.W. Negele and H. Orland, *Quantum Many-Particle Systems* (Addison-Wesley, Redwood, 1988)
- [8] G. Baym and N.D. Mermin, J. Math. Phys. **2**,232 (1961)
- [9] I. Dzyaloshinskii, Phys. Rev. B **68**, 085113 (2003)
- [10] J.M. Luttinger, Phys. Rev. **121**, 942 (1961)
- [11] M. Potthoff, Condens. Mat. Phys. **9**, 557 (2006)
- [12] M. Potthoff in A. Avella and F. Mancini (eds.): *Theoretical Methods for Strongly Correlated Systems* (Springer, 2011); see also preprint arXiv:11082183.
- [13] L. Hedin, Phys. Rev. **139**, A796 (1965)
- [14] N.E. Bickers, D.J. Scalapino, and S.R. White Phys. Rev. Lett. **62**, 961 (1989)